Analysis and Characterization of Shielding Material for Mitigating Electromagnetic Interference in UAVs

Yanuar Prabowo[1], Imas Tri Setyadewi [1*], Mohammad Amanta Kumala Sakti[1], Yomi Guno[1,2], Wahyudi[1], Donatina Miswati Hadiyanti[1], Novelita Rahayu[1,2], Nurul Lailatul Muzayadah[1], Cahya Edi Santosa[1]

[1] *Research Center for Aeronautics, Technology, National Research and Innovation Agency*
Jl. Raya LAPAN, Sukamulya, Rumpin, Bogor, Jawa Barat, Indonesia 16350
[2] *School of Electrical Engineering and Informatics (STEI), Bandung Institute of Technology (ITB), Bandung, Indonesia*
[*]*Corresponding author. Email: imas003@brin.go.id*

Abstract— This study aims to mitigate the impact of electromagnetic interference on the performance of electronic systems in Unmanned Aerial Vehicles (UAVs) by employing various shielding materials. The materials tested include carbon fiber, E-glass, E-glass with an aluminium foil, and E-glass with a copper foil. A Vector Network Analyzer (VNA) and scattering parameter (S-Parameter) analysis, including reflection, absorption, and multiple reflection, were used to evaluate the shielding effectiveness of these materials within the frequency range of 4 - 5 GHz. The results showed that E-glass coated with copper had good overall shielding performance for SER, SEA, and SET values. This material reached a SET value of 96 dB at a frequency of 4.6 GHz, followed by E-glass coated with aluminium. In addition, adding carbon layers increased the shielding effectiveness, while E-glass without coating had the lowest shielding performance compared to the other materials. These findings indicate that E-glass coated with metal provides superior shielding effectiveness compared to carbon fiber, even when used in greater thickness.

Keywords— E-glass; Shielding effectiveness; Carbon; Unmanned Aerial Vehicle; Reflection; Absorption.

I. INTRODUCTION

Unmanned Aerial Vehicles (UAVs) are rapidly advancing for civil and military purposes. The evolution of UAV applications is accompanied by increasing complexity in the payload and electronic systems they carry. During operation, the electromagnetic environment can impact the UAV's performance, whether from internal interactions between UAV components or external sources like lightning and electrical towers, potentially hindering optimal functionality. Electromagnetic Interference (EMI) refers to electromagnetic pollution caused by natural sources (e.g., lightning, solar radiation) or electronic equipment/circuits at the source frequency, which can degrade the quality and performance of electronic systems. Electromagnetic Compatibility (EMC), on the other hand, is the ability of a material to function effectively in an electromagnetic environment without being influenced by or causing interference to its surroundings [1].

UAVs typically have limited compartments that must accommodate various payloads specific to their flight missions. One critical component is the data link system, which is intricately integrated within the UAV's compartment along with other electronic components such as sensors, power, and communication systems. This data link system is essential for facilitating information transmission between the Ground Control Station (GCS) and the UAV. The constrained space within the UAV compartment significantly increases the risk of electromagnetic interference. Therefore, it is crucial to protect the UAV's components and systems from electromagnetic interference to ensure the safety of the air platform and the optimal performance of the aircraft. [2]. The risk of failure in UAVs is higher because some of their structures are made from composite materials such as carbon fiber, glass fiber, aramid, and ABS materials [3] - [6].

Shielding is an effective strategy to mitigate the effects of Electromagnetic Interference (EMI). It can significantly reduce the transmission of electromagnetic wave energy, isolate and attenuate the interference affecting electronic devices, and block interference propagation paths to protect these devices [7]. Several studies have been conducted on shielding effectiveness. Karahan (2025) studied polymer matrix composites (PMCs) with cold spray metallization, which have been carried out to reduce EMI, however their overall shielding effectiveness is still limited compared to metallic materials [8]. Mi Zhou compares different shielding methods for multicore cables, focusing on their effectiveness in reducing lightning surge currents, and evaluates the shielding and cable core coating methods [9].

Shielding materials can reduce transmitted signals through reflection from the wave field, absorption, and power dissipation within the material [10]. Various alternatives and innovations in materials have been explored to mitigate the effects of EMI and enhance material effectiveness against electromagnetic fields across different frequency ranges, including carbon and fiberglass materials [11]. A recent study presents significantly high shielding effectiveness by using ultrathin and lightweight carbon nanotube (CNT). Yongho studied single walled carbon nanotube (SWCNT) in the X band frequency range and achieved an EMI SE of 55,53 dB [12]. Another, experiment conducted was done by Yiyou, using carbon nanotubes and graphene composite film with covalent bonds (CNT-gGf). It achieved an excellent conductivity of 1300 S cm^{-1}, which surpasses that of pure graphene film and

Received 23 August 2024, Revised 3 October 2025, Accepted 4 October 2025.
DOI: https://doi.org/10.15294/jte.v17i1.12588

gives outstanding electromagnetic shielding (EMI) exceeding 55 dB with a thickness of 20 µm [13].

While these results highlight the potential of advanced nanomaterials, our work focuses on E-glass combined with copper and aluminium foils, which represents a more practical and cost-effective approach for UAV applications. Compared to CNT or graphene, which remain relatively expensive and complex to fabricate at larger scales, E-glass with metallic coatings offers a feasible solution that can be more readily implemented in actual UAV structures. This study aims to investigate and evaluate the effectiveness of carbon-based materials and E-glass with different compositions and variations in addressing EMI in UAVs. Carbon materials will be varied by the number of layers, ranging from 1 to 5. E-glass materials will be varied by adding layers of aluminium and copper. The application of aluminium and copper foil to the specimen layer is a new development in this research. The material will be examined at frequencies between 4 GHz and 5 GHz. This frequency band is employed to transmit real-time video payload data from the UAV to the GCS.

II. METHOD

The shielding effectiveness of electromagnetic interference protection (EMI SE) is the ability to reduce electromagnetic radiation generated by EMI sources. EMI Shielding Effectiveness (SE) is the ratio between incident field strength and transmitted field strength. This SE is expressed using a logarithmic scale in decibel units (dB) with the equation [14]:

$$SE_P = 10 \log (P_{in}/P_{out}) \quad (1)$$

$$SE_E = 20 \log (E_{in}/E_{out}) \quad (2)$$

$$SE_H = 20 \log (H_{in}/H_{out}) \quad (3)$$

Where P, E, and H in equations (1), (2), and (3) are the strength of the plane wave, electric field, and magnetic field, respectively, from the Electromagnetic (EM) wave. The subscripts in and out indicate the field strength incident upon and transmitted through the EMI shielding material, respectively. The shielding effectiveness is expressed in decibels (dB) [14].

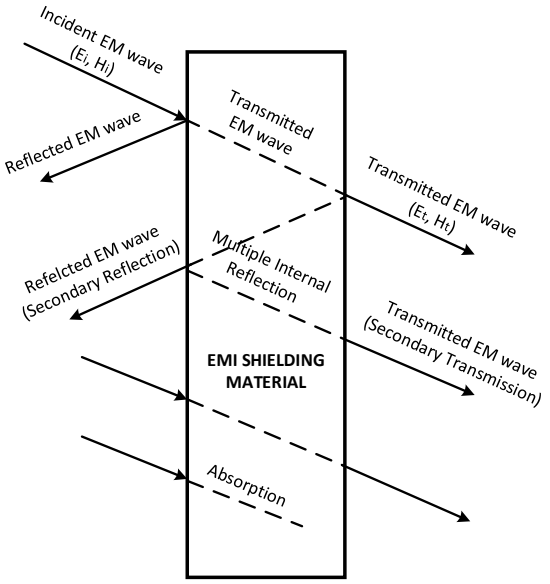

Figure 1. EMI Shielding mechanism [15]

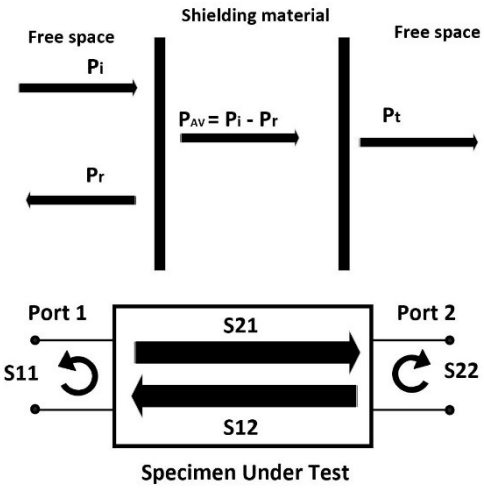

Figure 2. Two-port scattering parameter [15]

Electromagnetic Interference Shielding Effectiveness (EMI SE) from a material has three mechanisms, namely reflection, absorption, and multiple reflection. These three mechanisms are significantly influenced by the type and thickness of the material, as the ratio of the incident field strength that passes through the material can result in the phenomena of reflection (R), absorption (A), and transmission (T) in electromagnetic waves. An illustration of this principle is shown in Figure 1.

When electromagnetic (EM) waves approach the surface of a shielding material with an intrinsic impedance different from the impedance of the medium through which the EM waves travel, they are reflected away from the surface and are also transmitted into the material. The impedance of the medium and material determines the strength of the waves reflected and transmitted.

To calculate the magnitude of EMI SE, an approach using a scattering parameter can be used. In an experiment, the behaviour of wave propagation through a material sample can be measured by a Vector Network Analyzer (VNA). The reflected and transmitted waves in a two-port VNA can be represented by the scattering parameter (S-parameter). An illustration of the scattering parameter is shown in Figure 2.

In the illustration of Figure 2, the parameters of the reflection (R) and transmission (T) signal can be calculated with the equation [15]:

$$R = \frac{P_r}{P_i} = \left|\frac{E_r}{E_i}\right|^2 = |S_{11}|^2 = |S_{22}|^2 \quad (4)$$

$$T = \frac{P_t}{P_i} = \left|\frac{E_t}{E_i}\right|^2 = |S_{21}|^2 = |S_{12}|^2 \quad (5)$$

P_i refers to power incident, P_r refers to power reflection, P_t refers to power transmission, P_{AV} refers to power available, S_{11} and S_{22} refer to the reflection coefficients measured at ports 1 and 2, respectively. The S_{21} and S_{12} coefficient corresponds to the amount of energy transmitted through the material, thus illustrating the shielding properties of the absorber [16], [17]. Where E_i, E_r, and E_t are the intensities of the incident, reflected, and transmitted waves. According to the law of power balance, the corresponding power coefficients of reflectivity (R), absorptivity (A), and transmissivity (T) satisfy the relation [15] :

$$R + A + T = 1 \quad (6)$$

According to the Schelkunoff theory, EMI SE is defined as the sum of three terms: reflection loss (SER), absorption loss

(SEA), and multiple reflection loss (SEm). It can be calculated by the S-Parameter approach of equations (4), (5), and (6) as follows [15]:

$$SE_T\ (dB) = SE_R + SE_A + SE_M \quad (7)$$

$$SE_R = 10log_{10}\left(\frac{P_i}{P_{AV}}\right) = 10log_{10}\left|\frac{1}{1-R}\right| = 10log_{10}\left|\frac{1}{1-{S_{11}}^2}\right| \quad (8)$$

$$SE_A = 10log_{10}\left(\frac{P_{AV}}{P_t}\right) = 10log_{10}\left|\frac{1-R}{T}\right| = 10log_{10}\left|\frac{1-{S_{11}}^2}{{S_{21}}^2}\right| \quad (9)$$

$$SE_T = 10log_{10}\left|\frac{1}{1-{S_{21}}^2}\right| \quad (10)$$

SE_M represents internal reflection in protective materials, usually for materials with a large surface area and thickness. When the total SE is greater than 15dB, the SE_M can be ignored [18].

In this research, the specimens were fabricated using the hand layup method. The study consisted of two main steps: producing composite specimens and testing them using a Vector Network Analyzer (VNA) with a specific test configuration. The measured S-parameter values were analyzed to evaluate the shielding effectiveness of the specimens.

A. Shield Material Specimen Design

The materials used in this study consist of three types, namely UD carbon fiber, E-glass 135 fiber, and E-glass 135 fiber, which are shielded by a copper layer with a layer arrangement and thickness that can be seen in Table I.

The fibers are laminated with a different number of layers so that they become composite specimens. The material composite specimen is made using the hand layup method by applying vinyl ester resin. This method was chosen because the process is simpler and is often used for UAV manufacturing. Due to the hand layup fabrication process, variations in thickness and uniformity may occur as a result of resin pooling, trapped air, and manual pressure.

TABLE I. COMPOSITE LAYER SPECIMEN

No	Composite Process	Specimen	Thickness (mm)	Layer
1	Lamination	Carbon UD	0.5	1 layer
2	Lamination	Carbon UD	0.9	2 layer
3	Lamination	Carbon UD	1.2	3 layer
4	Lamination	Carbon UD	1.4	4 layer
5	Lamination	Carbon UD	1.8	5 layer
6	Lamination	E-Glass 135	1.2	3 layer
7	Lamination	E-Glass 135	1.2	3 layers + 1 layer copper and aluminium foil

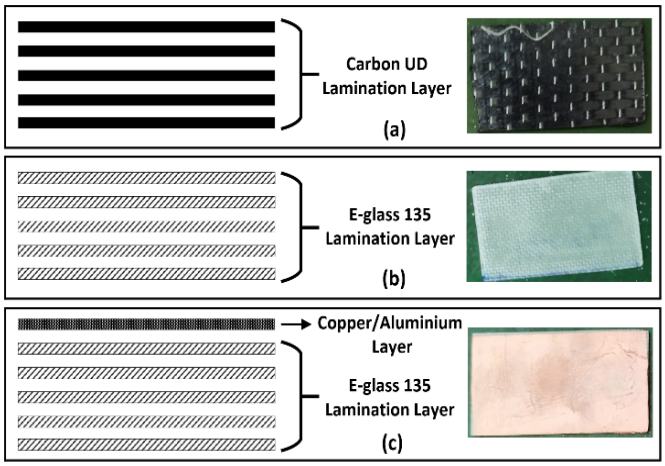

Figure 3. Composite Specimen Laminate Configuration:(a) Carbon UD, (b) E-glass 135, (c) E-glass 135 with aluminium or copper foil.

According to ASM literature, hand layup composites usually exhibit a thickness variation of ±5–10%. The measurements of the fabricated samples in this study were found to fall within this tolerance range [19]. The configuration of the laminate from the composite material can be seen in Figure 3. Copper and aluminium foil were placed on the top layer of the E-glass 135 laminate. The thicknesses of the metallic foils were 0.10 mm for copper and 0.11 mm for aluminium. The dimensions of the specimens used in this research were 5.3 cm × 2.8 cm.

B. Testing Configuration

The device used to obtain the S-parameter value is a waveguide type WR-187 with a working frequency of 3.94 GHz to 5.99 GHz and a VNA Keysight N9917A. The waveguide was connected to the VNA using coaxial cables on ports 1 and 2. The test configuration can be seen in Figure 4. The material specimen was placed on the surface of the waveguide, from this measurement, the scattering parameter values would be obtained, namely S11, S22, S21, and S12.

The specimens were measured in the frequency range of 4–5 GHz. This frequency range was selected because one of the UAV telemetry systems operates at 4.4–4.8 GHz. Hence, it is necessary to protect the UAV's onboard system from radiation interference occurring in this frequency band.

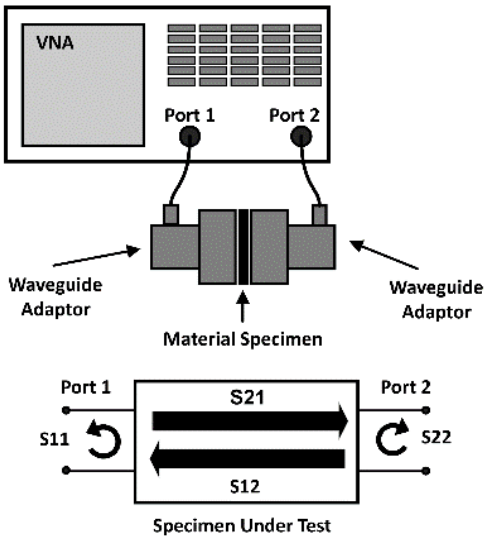

Figure 4. Testing configuration

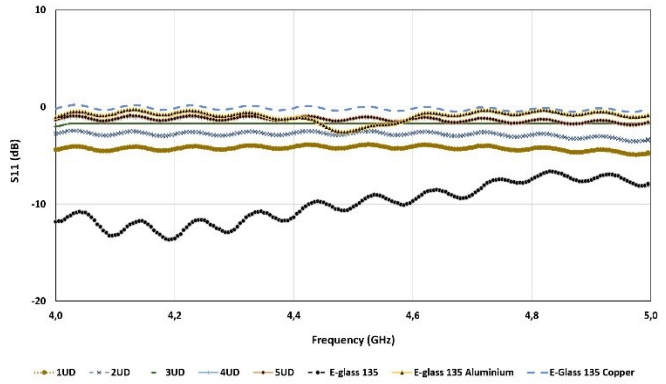

Figure 5. S11 parameter

III. Results And Discussion

S-parameters were obtained in the form of S11 and S21 for all samples of the tested material. The S11 parameter represents the reflection loss of the tested materials, as shown in Figure 5. The E-glass 135 material exhibits the lowest S11 values, ranging from 6 dB to 13 dB. This indicates that only a small portion of the power transmitted from port 1 is reflected, resulting in better transmission performance. In contrast, the other materials exhibit relatively high S11 values, ranging from -0.2 dB to -5 dB, which implies higher reflection and lower transmission efficiency.

The measurement results of S21 for various materials are illustrated in Figure 6. The S21 parameter represents the amount of power transmitted through the material, a lower S21 value indicates higher attenuation, while a higher value implies better transmission. From the measurements, the lowest S21 values are observed for E-glass 135 Copper, ranging from 50 dB to 78 dB, indicating that most of the transmitted power is attenuated, thereby providing excellent shielding effectiveness. In contrast, the highest S21 values are found in E-glass 135, with values ranging from 1.6 dB to 0.5 dB, suggesting that this material allows power to be transmitted more efficiently.

Electromagnetic interference SE is a measurement of a material's ability to reduce the intensity of EM waves and is expressed in decibels (dB). The analysis of the magnitude of reflection and insertion loss is obtained based on equations (8) and (9). Figure 7 shows a graph of the SER magnitude of the six samples as a function of frequency.

E-glass 135 material samples with copper shield showed the highest SER value, with a value close to 35.3 dB at a frequency of 4.5 GHz. While E-glass material had the lowest SER value around 0.344 dB at a frequency of 4.5 GHz. As expressed in equation (7), a higher S11 value corresponds to a higher SER. The second highest SER value was E-glass material with aluminium shield, and for carbon-based material from 1 to 5

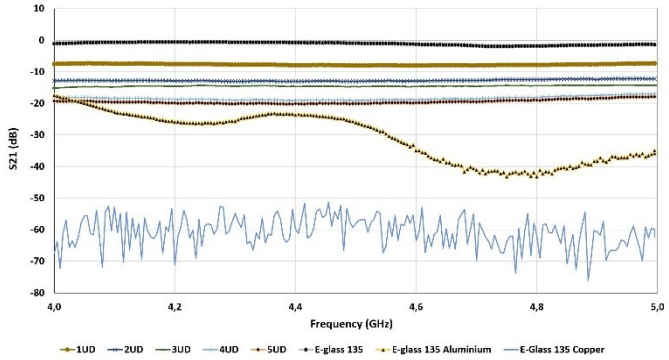

Figure 6. S21 parameter

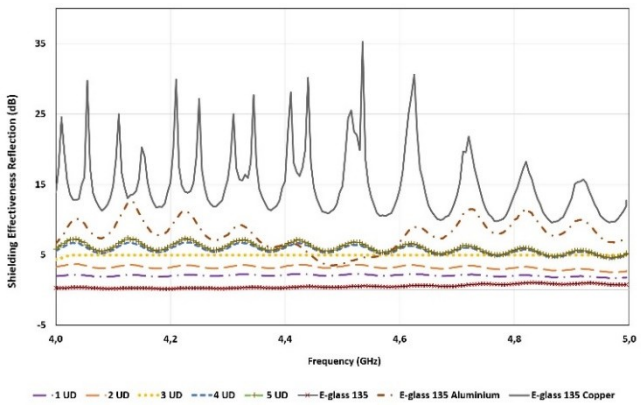

Figure 7. Shielding Effectiveness Reflection (SER)

layers had a SER value above E-glass material respectively. The results indicate that the addition of metallic shielding significantly enhances the shielding effectiveness. Furthermore, the carbon-based composites with one to five layers consistently achieved higher SER values than the E-glass 135, indicating that both material composition and layer number play critical roles in electromagnetic shielding performance.

A high SER value, as typically observed in metals with very high electrical conductivity, indicates that most of the incident electromagnetic energy is reflected rather than absorbed. In contrast, materials with lower conductivity, such as carbon laminates or E-glass exhibit lower SER values, meaning they tend to absorb or transmit more energy instead of reflecting it [20] - [22].

Figure 8 shows the magnitude of SEA material as a function of frequency. In the graph, the smallest SEA is in the E-glass 135 material. Then, with the increase in the thickness of the UD carbon material from 1 to 5 layers. E-glass material shielded with metal has a greater SEA value than carbon. E-Glass with aluminium layers has a SEA value that tends to be even greater with the increase in frequency, and the highest average value at a frequency of 4.6-4.8 GHz. The largest SEA value for the overall frequency in the range of 4 - 5 GHz is produced by the E-glass material with a copper layer with a value around 65 dB.

When viewed in the formulation of finding the SEA value as in equation (9), the decreases in absorption value of material or S21 as seen in Figure. 6, will increase the SEA value. So the material that has the smallest absorption value is E-Glass with a copper layer, most of the power is transmitted to produce the greatest SEA value reaching 75 dB at a frequency of 4.9 GHz.

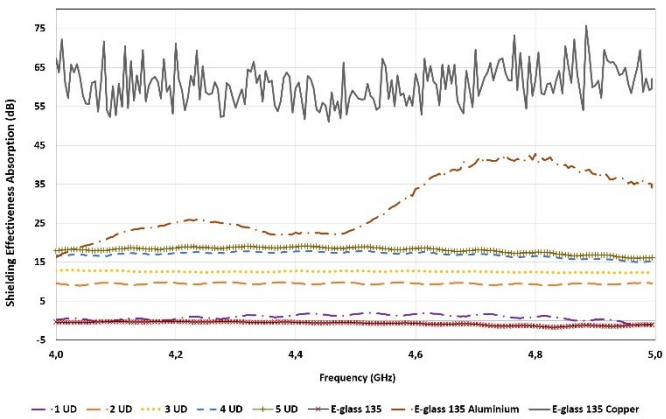

Figure 8. Shielding Effectiveness Absorption (SEA)

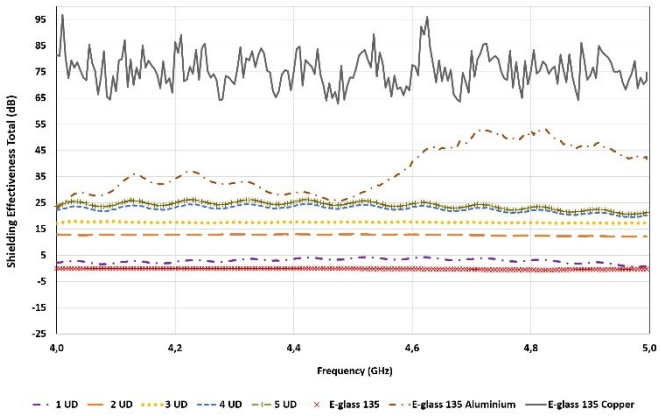

Figure 9. Shielding Effectiveness Total (SET)

Compared to metal type materials, carbon has a lower performance in terms of SEA. The E-glass specimen coated with copper exhibited a maximum SEA significantly higher than the five-ply carbon laminate with the same thickness.

Figure 9 shows the pattern of SET of materials like the SEA graph. This is due to the calculation of the amount of total shielding effectiveness based on equation (7) is the influence of the SEA and SER, where the component of the reflectivity is then lost so that the calculation set depends only on the S21 component or insertion loss. E-glass material with the lowest SER value has the smallest shielding effectiveness value, while copper-shielded E-glass material with the highest shielding effectiveness value reaches 96 dB at 4.6 GHz frequency.

Metal material has very high electrical conductivity so metals can efficiently direct and reduce electromagnetic signals. In addition, the presence of skin effects on high frequencies can cause current flow to be concentrated on the surface of the conductive material. This effect can occur on copper-shielded e-glasses because it has an ideal surface, making it possible to absorb and direct the electromagnetic signal well. When an electromagnetic wave encounters the metal surface, the free electrons generate strong induced currents that produce a counter-electromagnetic field, resulting in dominant reflection and thus a higher SER value. At the same time, the concentration of current near the surface at higher frequencies enhances the absorption component, which contributes to the high SEA [23], [24].

The carbon SET value is smaller than E-glass with copper shielding. This is because at higher frequencies, electromagnetic signals will produce greater energy which causes them to penetrate non-conductive materials such as carbon fibers more easily. The trend of signal leakage in carbon fiber is greater than in metal materials such as copper. The carbon SET value is smaller than E-glass with copper shielding. This is because at higher frequencies, electromagnetic signals will produce greater energy which causes it to penetrate non-conductive materials such as carbon fibers more easily. The propensity of signal leakage in carbon fiber is greater than in metal materials such as copper.

The higher SEA and SET values obtained in the E-glass with copper shielding can be attributed to its high electrical conductivity, which reduces skin depth and allows stronger attenuation of the incident wave. This indicates that the contribution of absorption is more dominant than reflection. In contrast, carbon fiber has lower conductivity and higher porosity, so part of the electromagnetic wave can leak through, especially at higher frequencies. These results show the trade-off between conductivity and absorption, and at the same time underline that using E-glass with metallic foils can be a more practical choice for UAV applications compared to more advanced but costly nanomaterials [16] [25].

IV. Conclusion

The variation of some shield materials has been measured. The highest SER value is obtained in E-glass material with copper shield with a value of 35.3 dB at a frequency of 4.5 GHz. Also, for SEA with a value of 75 dB at a frequency of 4.9 GHz. The SET value is strongly influenced by the SEA value, so the E-glass type material is copper shielded with the highest effectiveness for the frequency range of 4 -5 GHz with the highest value of 96 dB at a frequency of 4.6 GHz. The use of materials with metal-shielded e-glass is more effective in electromagnetic signal shields compared to carbon-type materials that have a greater thickness.

Acknowledgment

This research is supported by the Research Center of Aeronautics Technology - National Research and Innovation Agency (BRIN) which has provided funding support through the House of the Aeronautics and Space Research Organization (ORPA) program with the CFC-06 proposal number.

References

[1] I. T. Setyadewi and P. S. Priambodo, “Study and Analysis of Crosstalk Reduction in UAV Cabling by Using Various Cable Types,” *Evergreen*, vol. 9, no. 1, pp. 150–155, 2022, doi: 10.5109/4774232.

[2] Z. Zhang, Y. Zhou, Y. Zhang, and B. Qian, “Strong Electromagnetic Interference and Protection in UAVs,” *Electronics*, vol. 13, no. 2. 2024, doi: 10.3390/electronics13020393.

[3] D. R. Somolinos *et al.*, “Shielding Effectiveness Measurement of an UAV Simplified Demonstrator Through Low-Level Swept Field (LLSF) Test,” *IEEE Trans Electromagn Compat*, vol. 64, no. 5, pp. 1665–1673, Oct. 2022, doi: 10.1109/TEMC.2022.3202636.

[4] A. H. Wahyudi *et al.*, “Performance Analysis of PLA-Based EMI Shield Material for MALE UAV Application,” *Proceedings of the 2021 Asia-Pacific International Symposium on Electromagnetic Compatibility, APEMC 2021*, 2021, doi: 10.1109/APEMC49932.2021.9597203.

[5] R. Suresha, H. K. Sachidananda, B. Shivamurthy, N. K. Swamy, and S. Parasuram, “Mechanical and electromagnetic shielding properties of carbon fabric with graphene nanoplatelets reinforced epoxy composites,” *Sci. Rep.*, vol. 15, no. 1, p. 15735, 2025, doi: 10.1038/s41598-025-00634-x.

[6] R. K. Bheema, J. Gopu, K. Bhaskaran, A. Verma, M. Chavali, and K. C. Etika, “A review on recent progress in polymer composites for effective electromagnetic interference shielding properties - structures, process, and sustainability approaches,” *Nanoscale Adv.*, vol. 6, no. 23, pp. 5773–5802, 2024, doi: 10.1039/d4na00572d.

[7] P. Xu, Y. Di, X. Yao, and S. Yang, “Study on shielding effectiveness of metal shielding mesh of cable joint,” *6th IEEE Global Electromagnetic Compatibility Conference, GEMCCon 2020 - Proceeding*, Oct. 2020, doi: 10.1109/GEMCCON50979.2020.9456730.

[8] B. Karahan, I. Ozdemir, T. Grund, N. Hanisch, and T. Lampke, “Advancements in cold spraying for polymer matrix composites: enhanced LSP and EMI shielding performance — review and future directions,” *J. Mater. Sci. Mater. Eng.*, vol. 20, no. 1, p. 13, 2025, doi: 10.1186/s40712-025-00223-w.

[9] M. Zhou, Y. Guo, W. Zhao, L. Cai, J. Wang, and T. Yang, “Comparison of Shielding Effectiveness of Different Shielding Methods for Multi-Core Cable on Lightning Surge Current,” *IEEE Trans Electromagn Compat*, vol. 64, no. 5, pp. 1742–1749, Oct. 2022, doi: 10.1109/TEMC.2022.3200400.

[10] E. Mikinka and M. Siwak, “Recent advances in electromagnetic interference shielding properties of carbon-fibre-reinforced polymer composites—a topical review,” *J. Mater. Sci. Mater. Electron.*, vol. 32, no. 20, pp. 24585–24643, 2021, doi: 10.1007/s10854-021-06900-8.

[11] A. Fionov *et al.*, “Radio-Absorbing Materials Based on Polymer Composites and Their Application to Solving the Problems of Electromagnetic Compatibility.,” *Polymers (Basel).*, vol. 14, no. 15, Jul. 2022, doi: 10.3390/polym14153026.

[12] T. Nguyen et al., “Exceptional Electromagnetic Interference Shielding Using Single-Walled Carbon Nanotube/Conductive Polymer Composites Films with Ultrathin, Lightweight Properties,” Carbon N. Y., vol. 230, p. 119567, 2024, doi: 10.1016/j.carbon.2024.119567.

[13] Y. Yu et al., "Sandwich-structure CNT-graphene film with covalent bond for high-performance electromagnetic shielding and thermal management," Carbon N. Y., vol. 228, p. 119420, 2024, doi: https://doi.org/10.1016/j.carbon.2024.119420.
[14] M. S. Hareesh, P. Joseph, and S. George, "Electromagnetic interference shielding: a comprehensive review of materials, mechanisms, and applications," *Nanoscale Adv.*, vol. 7, no. 15, pp. 4510–4534, 2025, doi: 10.1039/d5na00240k.
[15] M. Peng and F. Qin, "Clarification of basic concepts for electromagnetic interference shielding effectiveness," J Appl Phys, vol. 130, no. 22, Dec. 2021, doi: 10.1063/5.0075019/158414.
[16] S. Zecchi *et al.*, "A Comprehensive Review of Electromagnetic Interference Shielding Composite Materials," *Micromachines (Basel)*, vol. 15, no. 2, 2024, doi: 10.3390/mi15020187.
[17] R. Kubacki, R. Przesmycki, and D. Laskowski, "Shielding effectiveness of Unmanned Aerial Vehicle Electronics with Graphene-Based Absorber," *Electronics (Switzerland)*, vol. 12, no. 18, 2023, doi: 10.3390/electronics12183973.
[18] J. Xiong *et al.*, "Multifunctional non-woven fabrics based on interfused MXene fibers," *Mater. Des.*, vol. 223, p. 111207, 2022, doi: https://doi.org/10.1016/j.matdes.2022.111207.
[19] D. B. Miracle et al., "ASM handbook," vol. 21, p. 3470, 2001.
[20] P. Clérico, X. Mininger, L. Prevond, T. Baudin, and A.-L. Helbert, "Magnetic shielding of a thin Al/steel/Al composite," *The International Journal for Computation and Mathematics in Electrical and Electronic Engineering*, vol. 2020, no. 3, doi: 10.1108/COMPEL.
[21] L. J. Chen, L. Xiao, L. Chen, and D. Zhao, "Research on a Metamaerial for electromagnetic protection of UAV," *2020 IEEE MTT-S International Microwave Workshop Series on Advanced Materials and Processes for RF and THz Applications, IMWS-AMP 2020 - Proceedings*, Jul. 2020, doi: 10.1109/IMWS-AMP49156.2020.9199702.
[22] M. Öztürk and D. Chung, "Enhancing the electromagnetic interference shielding effectiveness of carbon-fiber reinforced cement paste by coating the carbon fiber with nickel," *J. Build. Eng.*, vol. 41, p. 102757, May 2021, doi: 10.1016/j.jobe.2021.102757.
[23] S. S. Hota *et al.*, "Absorption-Dominant Electromagnetic Interference Shielding of Polymer Nanocomposite PVDF/LiNbO3 for High-Frequency Microwave Application," *ACS Appl. Electron. Mater.*, vol. 7, no. 10, pp. 4481–4492, May 2025, doi: 10.1021/acsaelm.5c00316.
[24] B. Park et al., "Absorption-Dominant Electromagnetic Interference (EMI) Shielding across Multiple mmWave Bands Using Conductive Patterned Magnetic Composite and Double-Walled Carbon Nanotube Film," Adv. Funct. Mater., vol. 34, no. 40, p. 2406197, 2024, doi: https://doi.org/10.1002/adfm.202406197.
[25] Q. Yang et al., "Advances in carbon fiber-based electromagnetic shielding materials: Composition, structure, and application," Carbon N. Y., vol. 226, p. 119203, Jun. 2024, doi: 10.1016/j.carbon.2024.119203.